ELSEVIER

Polymer 42 (2001) 8621–8627

polymer

www.elsevier.com/locate/polymer

Thermal and dynamic mechanical properties of metallocene polyethylene

M. Razavi-Nouri, J.N. Hay*

School of Metallurgy and Materials, The University of Birmingham, P.O. Box 363, Edgbaston, Birmingham B15 2TT, UK

Received 19 April 2001; received in revised form 16 May 2001; accepted 28 May 2001

Abstract

A comprehensive study has been made of a metallocene polyethylene (m-PE) characterising the isothermal crystallisation kinetics, melting and crystallisation behaviour, crystal growth and dynamic mechanical properties in order to understand the relationship between molecular structure and mechanical properties of this new class of polyethylene. The melting behaviour after step-wise crystallisation showed that m-PE consisted of molecular fractions with different molecular weight and branch distribution. Dynamic mechanical property studies showed that three transitions existed in m-PE with the α-transition increasing in intensity and shifting to higher temperatures in samples crystallised at higher temperature compared with rapidly cooled samples.

Keywords: Metallocene polyethylene; Differential scanning calorimeter; Crystallisation

1. Introduction

Production of ethylene/α-olefin copolymers by Ziegler–Natta (Z–N) catalysts to produce linear low density polyethylene (LLDPE) is difficult due to the much greater reactivity of the ethylene to polymerise than the α-olefin [1–7]. High yields of the LLDPE lead to wide variations in comonomer composition and with the heterogeneous nature of the Z–N catalyst with a range of active sites to very broad molecular weight distributions. Metallocene catalysts appear to be more homogeneous with a single site produce a more definable polyolefin with narrower molecular weight and comonomer distributions as well as closer control on side-chain length and degree of branching [8,9]. Metallocene catalysts generally have a transition element, usually from Group 4b, sandwiched between two cyclopentadienyl ring structures and this leads to some solubility of the catalyst in the polymerisation matrix. These catalysts have been used to produce a wide range of ethylene/α-olefin copolymers with α-olefin as octane-1 that have narrower molecular weight and comonomer distributions than the corresponding LLDPEs produced by the conventional Z–N catalysts. This makes them particularly useful as model systems in the study of the effect of molecular structure on the morphology and material properties of polyethylene [10]. Their flexibility, low temperature ductility, and thermoplastic elastomeric behaviour as well as lower hexane extraction properties of the new polyolefins make them useful in medical and packaging industries.

The present paper investigates the thermal and dynamic mechanical properties of a metallocene polyethylene to understand the effect of branch distribution on structure–property relationships in polyethylene.

2. Experimental

The metallocene polyethylene (m-PE) used was supplied by Exxon Chemical (France) as an Exact grade 3009. It is a copolymer of ethylene and hexane-1. Its melt flow index as measured by a Davenport MFI apparatus at 190°C and 2.160 kg load is 0.16 g min^{-1}. The number average molecular weight, M_n, weight average molecular weight, M_w and polydispersity are 40, 100 kg mol^{-1} and 2.5, respectively [11]. The density as measured by an immersion method is 0.923 g cm^{-3}. ^{13}C NMR spectroscopy showed that it contained an average of 4 mol% hexane-1 comonomer content [11]. Fractionation by temperature rising elution fractionation showed that this varied from 2 to 6 mol% across the sample.

Square sheets of m-PE (1.6 mm thick) were prepared from granules by pressing them between PTFE sheets in a hydraulic press at 160°C for 5 min. The sheets were quenched either directly into the water (water-cooled sample) or slow cooled in the hydraulic press to room temperature over 5 h (slow-cooled sample).

* Corresponding author. Tel.: +44-121-414-4544; fax: +44-121-414-5232.

E-mail address: j.n.hay@bham.ac.uk (J.N. Hay).

0032-3861/01/$ - see front matter
PII: S0032-3861(01)00377-9

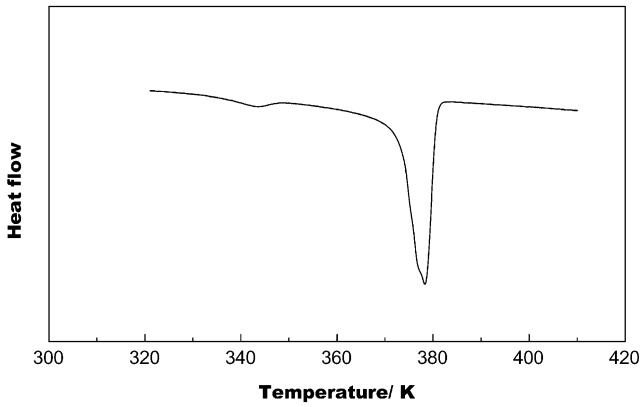

Fig. 1. The crystallisation temperature range of the m-PE on cooling.

Melting and crystallisation rate were measured using a Perkin–Elmer differential scanning calorimeter (model DSC-2) interfaced to a PC. The temperature scale of calorimeter was calibrated from the melting points of indium, tin and stearic acid and the thermal response from the enthalpy of indium.

The dynamic mechanical relaxation spectrum of the sample was measured using a Polymer Laboratories dynamic mechanical thermal analyser (DMTA) controlled by an IBM PS-2 computer. Rectangular samples ($40 \times 12.7 \times 1.6$ mm^3) were clamped in the measuring head on a steel frame supported by ceramic pillars. They were flexed in a dual cantilever mode by a central clamp driven sinusoidal by an electromagnetic vibrator through a ceramic drive shaft. The temperature was controlled using a Polymer Laboratories temperature programmer. Sub-ambient temperatures were achieved using liquid nitrogen purging through the DMTA jacket. The temperature range -150 to 300°C, heating rate of 1°C min^{-1} and frequency range from 0.01 to 100 Hz were used.

The spherulitic texture and radial growth rates were measured with a polarised light microscope (Leitz Dialux) fitted with a Linkam hot stage (TH600). The temperature of the stage was controlled with a temperature controller (PR600), working in the range of ambient to 773 K and with heating rates of 0.1–99 K min^{-1}. Calibration of hot stage was carried out using zone refined stearic and benzoic acid.

A scanning electron microscope (SEM), Jeol model 5410 was used to examine the spherulitic texture of the m-PE. Permanganic acid (7% potassium permanganate in concentrated sulphuric acid) was used to etch away the amorphous leaving crystalline regions. The etched sample after washing with water and acetone, was fixed on to an aluminium sample stub and sputtered with gold for examination in the SEM.

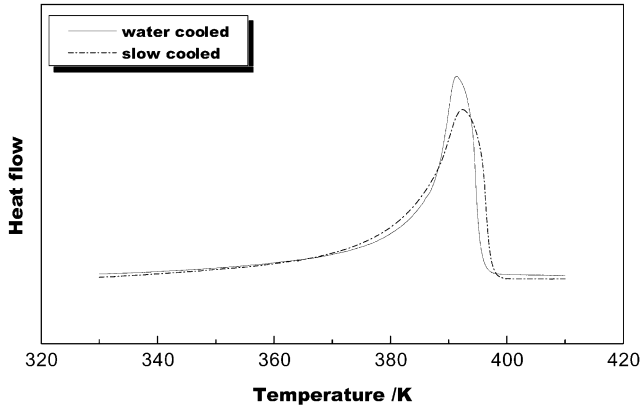

Fig. 2. The effect of slow and rapid cooling on the melting endotherm of m-PE.

3. Results and discussion

3.1. Melting behaviour and crystallisation rate studies of m-PE

Fig. 1 shows the temperature range over which m-PE crystallised on cooling at 2.5 K min^{-1}. Using heating rates of 2.5, 5 and 10 K min^{-1} and extrapolating to zero heating rate, the temperatures corresponding to the onset and maximum rate of crystallisation were found to be 386.5 and 383.3 K, respectively. The effect of cooling rate on the subsequent melting endotherms of m-PE can be seen in Fig. 2: lower rates broadened the melting endotherm and the temperature corresponding to the last trace of crystallinity increased consistent with crystallising at a higher temperature. The degree of crystallinity of the slow-cooled, as measured by DSC, were significantly greater than the water-cooled samples, i.e. $45 \pm 2\%$ compared with $40 \pm 2\%$. Isothermal crystallisation rates were measured in the temperature range 384–388 K consistent with these observations. For isothermal crystallisation from the melt, the extent of crystallinity, X_t, is related to time t by the Avrami equation [12–15] such that

$$1 - \frac{X_t}{X_\infty} = \exp(-Zt^n) \tag{1}$$

where Z is a composite rate constant incorporating nucleation characteristics and growth rate, n is the Avrami exponent, X_t and X_∞ are the volume fractions of crystallised material at time t and at infinitive. n adopts different values for different crystallisation mechanisms [12].

Accordingly,

$$\log\left[-\ln\left(1 - \frac{X_t}{X_\infty}\right)\right] = n \log t + \log Z \tag{2}$$

and also

$$n = -t\left(\frac{\mathrm{d}X_t}{\mathrm{d}t}\right)\left[\left(1 - \frac{X_t}{X_\infty}\right)\ln\left(1 - \frac{X_t}{X_\infty}\right)\right] \tag{3}$$

An average rate constant Z was calculated from the

Table 1
Crystallisation rate parameters

Crystallisation temperature (K)	Half-life, $t_{1/2}$ (s)	n value ± 0.2	Rate constant, Z ($\times 10^4$ min^{-n})
384.4	103	2.9	1446
384.9	131	2.8	779
385.4	187	2.8	287
385.7	273	2.8	100
386.2	303	2.9	63
387.1	589	2.9	9.2
388.1	1534	2.8	0.8

half-life, $t_{1/2}$, and the value of n at $t_{1/2}$, since

$$Z = \frac{\ln 2}{(t_{1/2})^n} \tag{4}$$

DSC was used to measure crystallisation rates as a function of time, assuming that the heat evolution was due solely to crystallisation, and the extent of crystallinity developed at time t could be determined by integrating the endotherms [16], i.e.

$$\frac{X_t}{X_\infty} = \frac{\int_0^t (\mathrm{d}H_t/\mathrm{d}t)\mathrm{d}t}{\int_0^\infty (\mathrm{d}H_t/\mathrm{d}t)\mathrm{d}t} \tag{5}$$

Table 1 lists the Avrami rate parameters determined for melt crystallisation of m-PE. The variation of half-life with temperatures is shown in Fig. 3. At all temperatures, the n value was 2.9 ± 0.2 consistent with the Avrami mechanism for growth of spherical particles from athermal nuclei, i.e. $n = 3.0$. It can be seen that the half-life increased rapidly with increasing crystallisation temperatures and that it approximately doubled in value for an increase in temperature of 1 K. This is commonly observed with polyethylene and severely limits the temperature range over which isothermal rates can be measured by DSC.

The observation of an increasing half-life with temperature is consistent with nucleation control of growth, and a dependence on the under-cooling from the equilibrium melting point, T_m^0. The temperature dependence of the isothermal crystallisation half-life as derived by Mandelkern [17] is

$$\ln\left(\frac{1}{t_{1/2}}\right) = A - \left(\frac{4\sigma\sigma_e}{R\Delta H T_c}\right)\left[\frac{(T_m^0)^a}{(T_m^0 - T_c)^a}\right] \tag{6}$$

where A is a constant, T_c is the crystallisation temperature, R is the gas constant, σ and σ_e are lateral and fold surface energies, ΔH is heat of fusion per monomer mole, and a is a constant such that $a = 1$ or 2 for primary or secondary nucleation. Fig. 4a and b shows the plots of $\ln(1/t_{1/2})$ according to $(T_m^0)^a/(T_m^0 - T_c)^a$. T_m^0 was taken to be 416 K and $\sigma = 0.1\Delta H$. Because of the restricted temperature range adopted in the DSC studies, no distinction could be made between the primary and secondary nucleation as the least

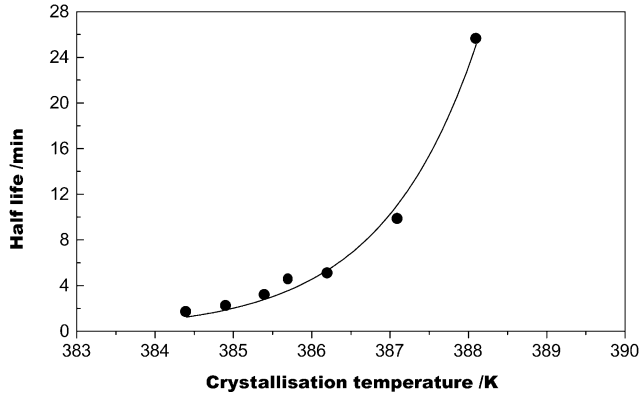

Fig. 3. The variation of the crystallisation half-life with temperature.

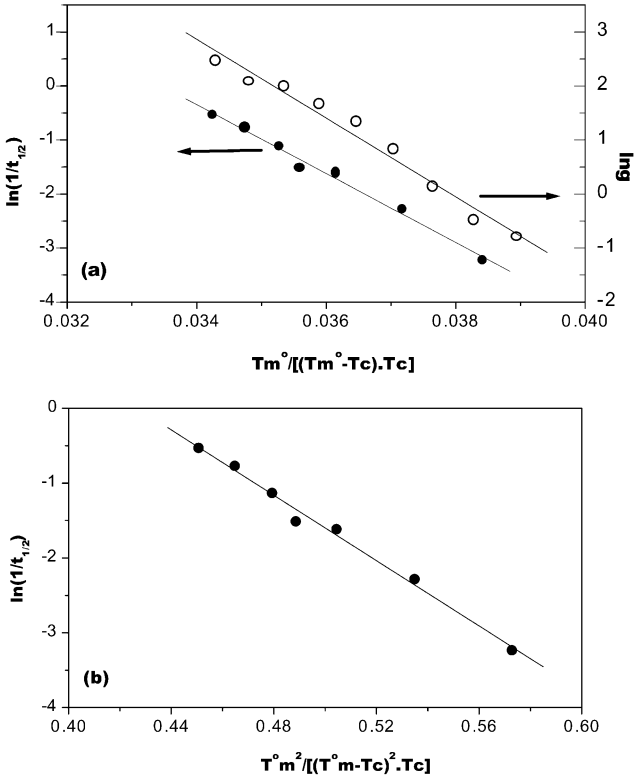

Fig. 4. Temperature dependence of crystallisation, (a) crystallisation half-lives and spherulite growth rates for $a = 1$, (b) crystallization half-lives for $a = 2$.

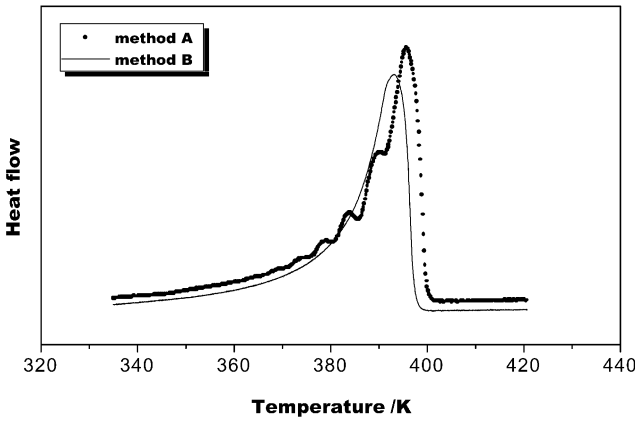

Fig. 5. Melting endotherms of m-PE, rate of heating 5 K min^{-1}.

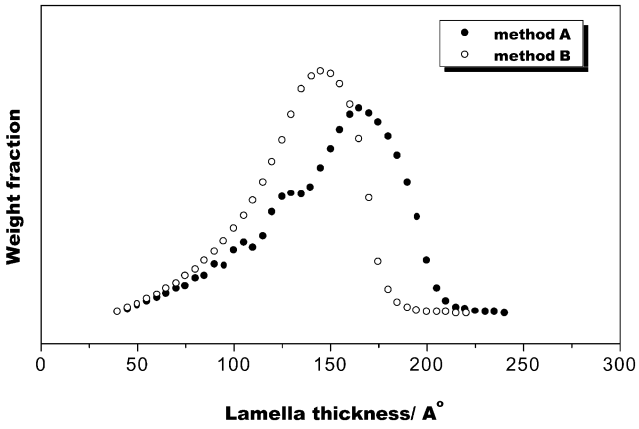

Fig. 6. Lamella thickness weight distribution.

square correlation coefficients were found to be same for both, see Fig. 4. The fold surface energy for $a = 1$ and 2 were 13 ± 2 and 0.5 ± 0.1 kJ mol^{-1}, respectively.

The distribution of lamella thickness has been measured from the melting endotherms using the relationship [18,19]

$$T_m = T_m^0\left(1 - \frac{2\sigma_e}{\Delta H l}\right) \tag{7}$$

where l is the lamellae thickness and ΔH is the melting enthalpy per unit volume. Weight, l_w, and number average, l_n, thicknesses were defined as

$$l_w = \sum_{i=1}^{i=n} l_i w_i \tag{8}$$

$$l_n = \frac{1}{\sum_{i=1}^{i=n} w_i/l_i} \tag{9}$$

$$\text{Polydispersity} = \frac{l_w}{l_n} \tag{10}$$

If butyl branches are excluded from the polyethylene crystals, then the melting endotherm, the lamellae distribution and the final degree of crystallinity which develops should reflect the long sequences of ethylene units between adjacent *n*-butyl branches along the chain. In order to check this proposition, m-PE was stepwise crystallised using two procedures, A and B. In A, m-PE was melted at 430 K for 5 min and the sample crystallised at decreasing temperatures, from 385 to 340 K in 5 K steps crystallising for 2 h and cooling between crystallisation temperatures at 160 K min^{-1}. The sample was then cooled to 320 K and subsequently heated at 5 K min^{-1} to 430 K to determine the melting range of the sample. In B, m-PE was melted at 430 for 5 min and then cooled at 10 K min^{-1} to 320 K. The sample was, then, heated at 5 K min^{-1} to 430 K. The DSC endotherms are shown in Fig. 5. Several well-resolved melting endotherms are present that could be attributed to the crystallisation of molecules with different amounts of hexane-1 comonomer throughout the polymer chains [20,21]. Fractionation by temperature rising elution fractionation (TREF) carried out by Feng [11] showed that several fractions could be separated between 70 and 115°C. Further characterisation revealed that although each fraction had a narrow molecular weight distribution, they contained different branch content, and in particular, the degree of branching decreased with increasing elution temperature. The broad melting endotherms from A and B are related to the molecular segregation by branch content that occurs during crystallisation. This allows the m-PE molecules that have sufficiently large sequence lengths between adjacent branch points to crystallise at the different temperatures during cooling. Using the extent of melting against temperature as determined by DSC, the lamella thickness distributions of the two samples were calculated using the analysis described in detail elsewhere [22]. It is apparent from Fig. 6 that procedure A leads to higher lamellar thickness but shows the effect of stepwise cooling and procedure B does not allow sufficient time for molecular segregation by branching to occur. Procedure B was modified to C, which allowed the sample to be cooled at 0.31 K min^{-1}. It was hoped that sufficient time would be allowed for the ethylene molecular sequences to segregate by size on cooling and that the subsequent melting endotherm would reflect the distribution of ethylene sequences in the copolymer. The melting endotherm and its analysis in terms of lamellar thickness are shown in Figs. 7 and 8. A more symmetrical distribution was observed by this method than either A or B, which more accurately reflects the ethylene sequence distribution in the copolymer.

3.2. Spherulitic growth rate

Polyethylene, in general, has a very high nucleation density and the spherulites diameters are too small to be resolved by light microscopy. Nucleation is heterogeneous and can be destroyed by over-heating. A thin film, 20 μm thick, of m-PE was heated at 340°C for 30 min and Fig. 9 shows a light micrograph of the spherulites observed on

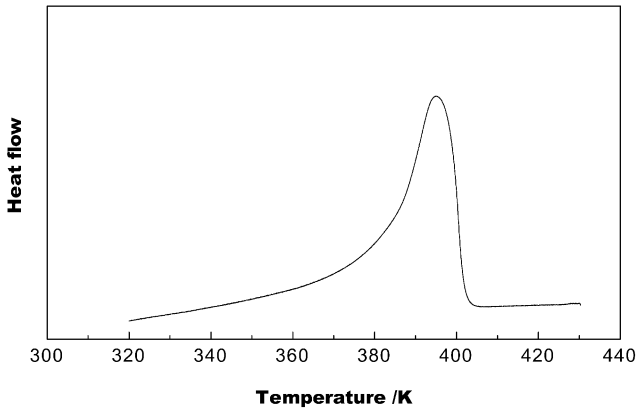

Fig. 7. Melting endotherm of slow cooled m-PE, rate of cooling 0.31 K min^{-1}, rate of heating 10 K min^{-1}.

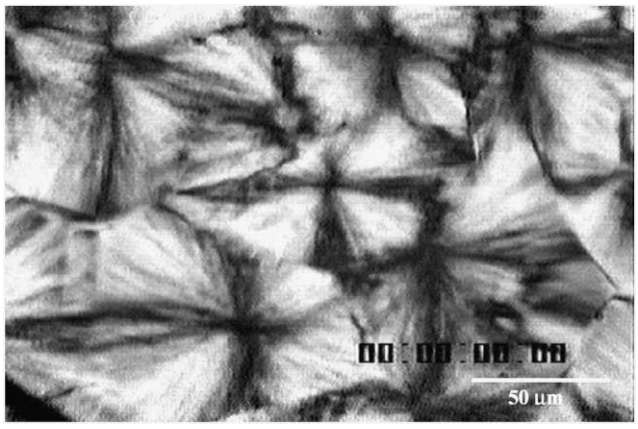

Fig. 9. Polarised light micrograph of m-PE spherulites, crystallised at 113.1°C after thermal treatment.

subsequent crystallisation at 113.1°C. It was not possible to resolve the spherulites diameters of the untreated crystalline m-PE by light microscopy. The material was birefringent but the particles were not resolvable. On etching these samples with permanganic acid, spherulites could be resolved in the SEM, and their diameters were on the average 5–10 μm, see Fig. 10. The presence of large spherulites, 50–100 μm in diameter, is attributed to a large reduction in nucleation density.

The radial growth was measured at various temperatures using a micrometer eyepiece. Plots of spherulite radius growth with time at each temperature, see Fig. 11, were linear from which the radial growth rates, g, were determined. The decrease with increasing temperature, see Fig. 12, was consistent with nucleation controlled growth and it followed the same dependence as the half-lives on reciprocal super-cooling as implied by Eq. (6), see Fig. 4a. The temperature dependence also gave a fold surface free energy of 13 ± 2 kJ mol^{-1} as observed previously.

The Avrami composite rate constant for growth of a spherical particle,

$$Z = \left(\frac{\pi}{3X_c}\right)\left(\frac{\rho_c}{\rho_l}\right)Ng^3 \tag{11}$$

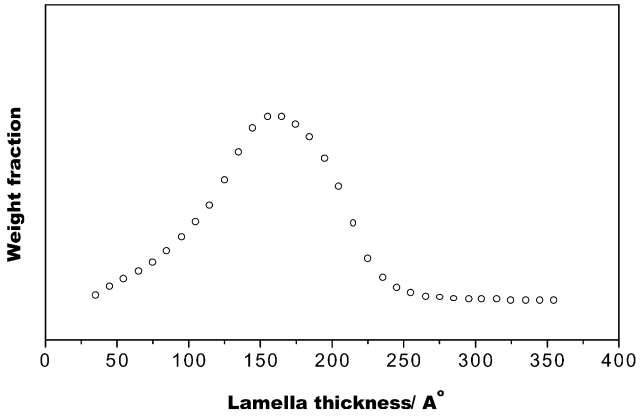

Fig. 8. Lamella thickness weight distribution of slow cooled m-PE.

where X_c is the degree of crystallinity of the sample, ρ_c and ρ_l are the densities of crystalline and amorphous material, N is the nucleation density and g is the radial growth rate. The nucleation density was calculated to be in the range of $0.1–0.4 \times 10^9$ nuclei cm^{-3}. This is consistent with the SEM observations that the spherulitic diameters were about 5–10 μm in the untreated m-PE samples.

3.3. Dynamic mechanical behaviour

Fig. 13 shows the variation in loss tangent of m-PE with temperature at 1 Hz. Three distinct transitions, corresponding to maxima in the loss tangent, can be seen. These are labelled as α, β, and γ in order of decreasing temperature. In m-PE, the α-transition was observed in the temperature range 20–100°C with a maximum in tan δ at 63°C. The molecular mechanism of this relaxation in PE is quite complex [10,23] and Boyd has attributed it to the deformation of amorphous regions as a result of reorientation within the crystallites [24]. He believes that the mobility of crystal stem leading to reorganisation of folds, cilia and intercrystalline links existed in the amorphous layer. However, Khanna et al. [25] have stated that deformation of chain

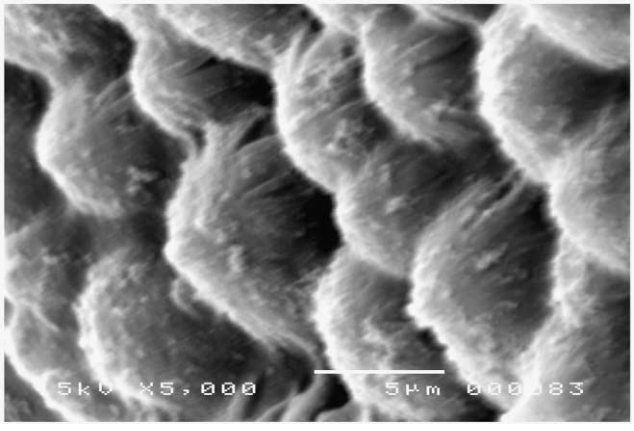

Fig. 10. Electron micrograph of etched m-PE, crystallised at 116.5°C.

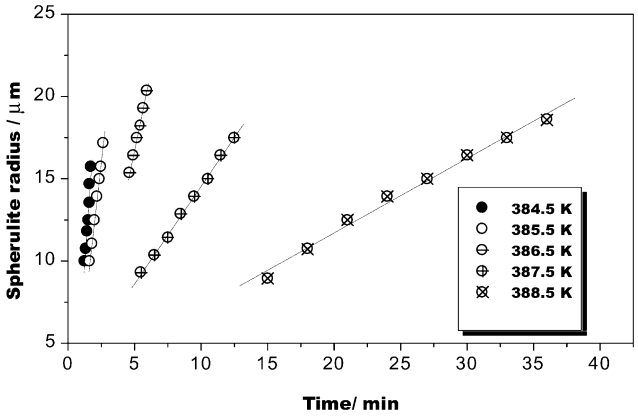

Fig. 11. Increase in spherulite's radius with time.

segments within the folds and loops of the interfacial region is responsible for the α-transition. Mandelkern [26] has shown that the position of the α-peak is inversely related to the lamella thickness in the crystalline section and its intensity increases with the degree of crystallinity.

The β-transition was observed in the temperature range −50 to 20°C with a maximum in tan δ at −10°C. Because of the low density the transition is barely discernable as a shoulder on the α-transition. This transition is strongly dependent on PE density [10] and as the density increases, the intensity of transition is reduced shifting also to higher temperatures. Above 0.92 g cm^{-3} the β-transition merges into the α-transition. Since, the β-transition can also be seen as a very weak transition in linear polyethylene, it is not related to the motions of branch carbons and Mandelkern [26] considers that it results from the motion of disordered chain units in the interfacial regions of semi-crystalline polymer and copolymers. The γ-transition of m-PE occurred at −112°C.

The effect of crystallinity and lamellar thickness on the transition temperatures were studied by cooling m-PE from the melt at different rates, see Fig. 14. The α-transition intensity increased and shifted to higher temperature with the more crystalline slow cooled samples. However, the position and intensity of the β-transition did not change significantly.

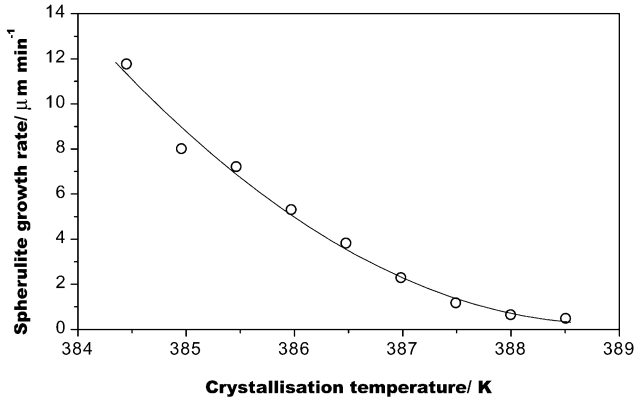

Fig. 12. Variation of radial growth rate with crystallisation temperature.

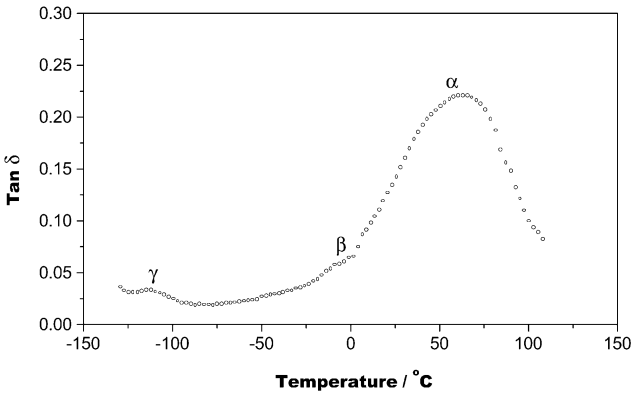

Fig. 13. Variation of the loss tangent of m-PE with temperature at 1 Hz.

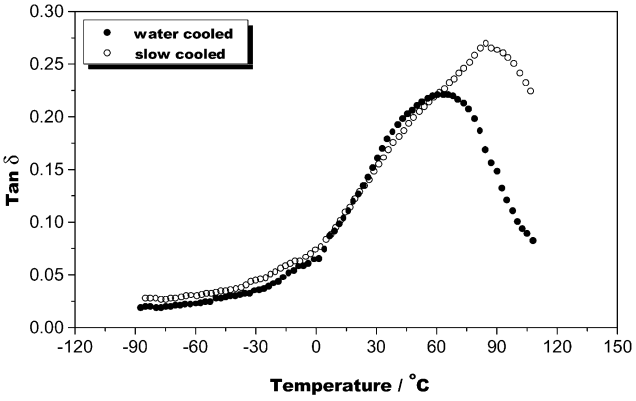

Fig. 14. Effect of cooling on the loss tangent of m-PE at 1 Hz.

4. Conclusion

The thermal, dynamic mechanical behaviour and morphology of a m-PE have been investigated. Step-wise crystallised m-PE melting curve shows that the m-PE consists of molecules with different branch content and stem length distribution, which allow each to crystallise at a certain temperature.

Dynamic mechanical studies indicate that the m-PE has three different transitions. α-transition increases and shifts to the higher temperature for slow-cooled sample compared to water-cooled sample. This is because of the higher degree of crystallinity and lamellar thickness of slow-cooled sample.

Acknowledgements

The authors wish to thank Mr Frank Biddlestone for his technical support and assistance and the Iranian Ministry of Culture and Higher Education and the Iran Polymer Institute

for the award of a scholarship to M.R.-N. during the tenure of this work.

References

[1] Yoon JS, Lee DH, Park ES, Lee IM, Park DK, Jung SO. Polymer 2000;41:4523.
[2] Bushick RD. J Polym Sci, Part A 1965;3:2047.
[3] Burfeld DR, Kachiwa N. Macromol Chem 1985;186:2657.
[4] Kimura K, Shigomura T, Yusasa S. J Appl Polym Sci 1984;29:3161.
[5] Wild L, Rye TR, Knobeloch DC, Peat IR. J Polym Sci, Polym Phys 1982;20:441.
[6] Nakano S, Goto Y. J Appl Polym Sci 1981;26:4217.
[7] Bergtrom C, Arena E. J Appl Polym Sci 1979;23:163.
[8] Scheirs J, Kaminsky W, editors. 1st ed. Metallocene-based polyolefins, vol. 2. Chichester: Wiley, 2000.
[9] Benedikt GM, Goodall BL, editors. Metallocene catalysed polymers — materials, properties, processing and markets. 1st ed. New York: Plastics Design Library, 1998.
[10] Woo L, Ling MTK, Westphal SP. Thermochim Acta 1996;272:171.
[11] Feng Y. PhD Thesis. University of Birmingham; 1997.
[12] Evans UR. Trans Faraday Soc 1945;41:365.
[13] Avrami M. J Chem Phys 1939;7:1103.
[14] Avrami M. J Chem Phys 1940;8:212.
[15] Avrami M. J Chem Phys 1941;9:177.
[16] Hay JN, Fitzgerald PA, Wiles M. Polymer 1976;17:1015.
[17] Mandelkern L, Fatou JG, Howard GC. J Phys Chem 1965;69:956.
[18] Zhou XQ. PhD Thesis. University of Birmingham; 1993.
[19] Young RJ. Introduction to polymer. New York: Chapman & Hall, 1987.
[20] Schontenden P, Piekel C, Koch M, Groenickx G, Reynners H. Polym Bull 1985;13:533.
[21] Schontenden P, Groenickx G, Vandes Heijdan B, Jansen F. Polymer 1987;28:2099.
[22] Mills PJ, Hay JN. Polymer 1984;25:1771.
[23] Clas SD, Mcfaddin DC, Russell KE. J Polym Sci, Polym Phys 1987;25:1057.
[24] Boyd RH. Polymer 1985;26:1123.
[25] Khanna YP, Turi EA, Taylor TJ, Vickroy VV, Abbott RF. Macromolecules 1985;18:1302.
[26] Popli R, Glotin M, Mandelkern L, Benson RS. J Polym Sci, Polym Phys 1984;22:407.